Better Sampling Bounds for Restricted Delaunay Triangulations and a Star-Shaped Property for Restricted Voronoi Cells

Jonathan Richard Shewchuk
University of California, Berkeley, CA, USA

Abstract

The restricted Delaunay triangulation of a closed surface Σ and a finite point set $V \subset \Sigma$ is a subcomplex of the Delaunay tetrahedralization of V whose triangles approximate Σ. It is well known that if V is a sufficiently dense sample of a smooth Σ, then the union of the restricted Delaunay triangles is homeomorphic to Σ. We show that an ϵ-sample with $\epsilon \leq 0.3245$ suffices. By comparison, Dey proves it for a 0.18-sample; our improved sampling bound reduces the number of sample points required by a factor of 3.25. More importantly, we improve a related sampling bound of Cheng et al. for Delaunay surface meshing, reducing the number of sample points required by a factor of 21. The first step of our homeomorphism proof is particularly interesting: we show that for a 0.44-sample, the restricted Voronoi cell of each site $v \in V$ is homeomorphic to a disk, and the orthogonal projection of the cell onto $T_v\Sigma$ (the plane tangent to Σ at v) is star-shaped.

2012 ACM Subject Classification Theory of computation → Computational geometry

Keywords and phrases Restricted Delaunay triangulation, restricted Voronoi diagram, surface sampling, surface mesh generation, surface reconstruction, ϵ-sample, homeomorphism

Digital Object Identifier 10.4230/LIPIcs.SoCG.2026.90

Related Version *Full Version*: `https://arxiv.org/abs/2603.19826` [32]

Funding Supported by the National Science Foundation under Award CCF-1909204.

Acknowledgements I thank Nina Amenta, Jean-Daniel Boissonnat, Siu-Wing Cheng, Tamal Dey, Arijit Ghosh, and Marc Khoury for discussions about surface sampling; and INRIA Sophia-Antipolis and the Geometrica Group, where this work began, for their kind reception during my 2010 sabbatical.

1 Introduction

The *restricted Delaunay triangulation* (RDT) is a well-established way of generating good-quality triangulations on curved surfaces [23]. Researchers have developed a theory of surface sampling to determine how we should sample points on a surface to guarantee that an RDT (or a related triangulation) is a topologically correct and geometrically accurate approximation of the surface [1, 2, 3, 6, 10, 12, 13, 14, 15, 17, 16, 18, 20, 23, 24, 26, 31, 34, 35]. RDTs and this surface sampling theory have equipped geometers to rigorously prove the correctness of algorithms for surface reconstruction [20] and surface mesh generation [18].

Think of the RDT as a function that takes in two inputs: a smooth, closed (compact with no boundary) surface $\Sigma \subset \mathbb{R}^3$ and a finite set $V \subset \Sigma$ of points, called *sites* (or *vertices* of the RDT). The set V is a *sample* or a *point cloud*. The output is a simplicial complex $\mathcal{T}$ whose vertices are V. The RDT $\mathcal{T}$ is a subcomplex of the three-dimensional Delaunay triangulation $\mathrm{Del}\, V$, but in typical usage $\mathcal{T}$ contains no tetrahedra; only triangles, edges, and the vertices V.

If V is sufficiently dense, $\mathcal{T}$ is a (topological) *triangulation* of Σ, which means that the *underlying space* of $\mathcal{T}$, written $|\mathcal{T}| = \bigcup_{\tau \in \mathcal{T}} \tau$, is homeomorphic to Σ. This paper proves that a modest sampling requirement suffices to guarantee that homeomorphism.

What does it mean for V to be "sufficiently dense"? Intuitively, there should be no large unsampled bare spots on Σ. Ideally, sampling requirements are adaptive, as a denser spacing of sites is needed in regions where Σ has higher curvature or closely-spaced "parts" like fingers on a hand, but simple regions need few sites. Many provably good algorithms for surface reconstruction assume that V is a so-called ϵ-sample of Σ (defined in Section 2), an adaptive sample in which a smaller ϵ implies more sites, closer together.

One main result of this paper is that if V is a 0.3245-sample of Σ, the underlying space of the RDT is homeomorphic to Σ. Dey [20] proved the same for a 0.18-sample. The new result reduces the number of sample points required by a factor of 3.25 (the square of 0.3245/0.18). Some well-known surface reconstruction algorithms such as the Crust [1] and Cocone [3] algorithms rely on identifying a superset of the RDT's triangles then paring them down. Any substantial relaxation of their sampling requirements is good news for a broad swath of existing algorithms, and it helps to explain why they work well in practice.

As a point of comparison, Bjerkevik [5] shows that no proof will ever guarantee homeomorphism for 0.72-samples, as there exist 0.72-samples with multiple, topologically different, correct reconstructions. (This limitation holds also for smooth, closed curves in the plane.)

We define another adaptive sampling condition better suited to mesh generation, enabling stronger sampling bounds: we prove homeomorphism for what we call a 0.4132-*Voronoi sample*. Cheng et al. [18] proved the same for a 0.09-Voronoi sample; our result reduces the number of sample points required by a factor of 21. Our bound implies better sampling bounds for existing surface meshing algorithms; it is this paper's most important result.

Also of interest are the new techniques introduced here to obtain these bounds. In particular, for a 0.44-sample or a 0.78-Voronoi sample, the restricted Voronoi cell of each site $v \in V$ (defined in Section 2) is homeomorphic to a disk. Moreover, let $T_v\Sigma$ denote the plane tangent to Σ at v; the orthogonal projection of v's cell onto $T_v\Sigma$ is *star-shaped*: a union of (infinitely many) line segments terminating at v. It seems a bit surprising that restricted Voronoi cells are better behaved with respect to coarse samples than restricted Voronoi vertices or edges, because the proofs by Dey [20] and Cheng et al. [18] use the soundness of the restricted Voronoi edges to establish the soundness of the restricted Voronoi cells. This paper reverses that sequence and, in my opinion, gets at the heart of the reasons why a restricted Voronoi cell is nicely shaped. Remarkably, the results about the Voronoi cells generalize to manifolds of higher dimension embedded in higher-dimensional spaces with no degradation in the bounds [32], although the homeomorphism result does not and cannot generalize to higher dimensions [16, 11, 9].

Not everyone gets excited by improved constants, but I advocate for the importance of tighter sampling theory for computational geometry – just as numerical analysts have devoted much effort to improving constants associated with quadrature rules, interpolation theory, and more. Strong bounds show that RDTs are useful, not merely theoretical.

2 Restricted Delaunay triangulations and ϵ-samples

The RDT is defined by dualizing a *restricted Voronoi diagram*, which will be our main object of study. Let $|pq|$ denote the Euclidean distance from p to q; equivalently, the length of the line segment pq. Given a closed surface $\Sigma \subset \mathbb{R}^3$ and a sample $V \subset \Sigma$, the *restricted Voronoi cell* of a site $v \in V$ is $\mathrm{Vor}|_\Sigma v = \{p \in \Sigma : |pv| \leq |pw| \text{ for all } w \in V\}$. Equivalently, $\mathrm{Vor}|_\Sigma v = \Sigma \cap \mathrm{Vor}\, v$, where $\mathrm{Vor}\, v$ is v's standard Voronoi cell in $\mathbb{R}^3$. The name "restricted Voronoi cell" means that $\mathrm{Vor}|_\Sigma v$ is the restriction of $\mathrm{Vor}\, v$ to the surface Σ. See Figure 1.

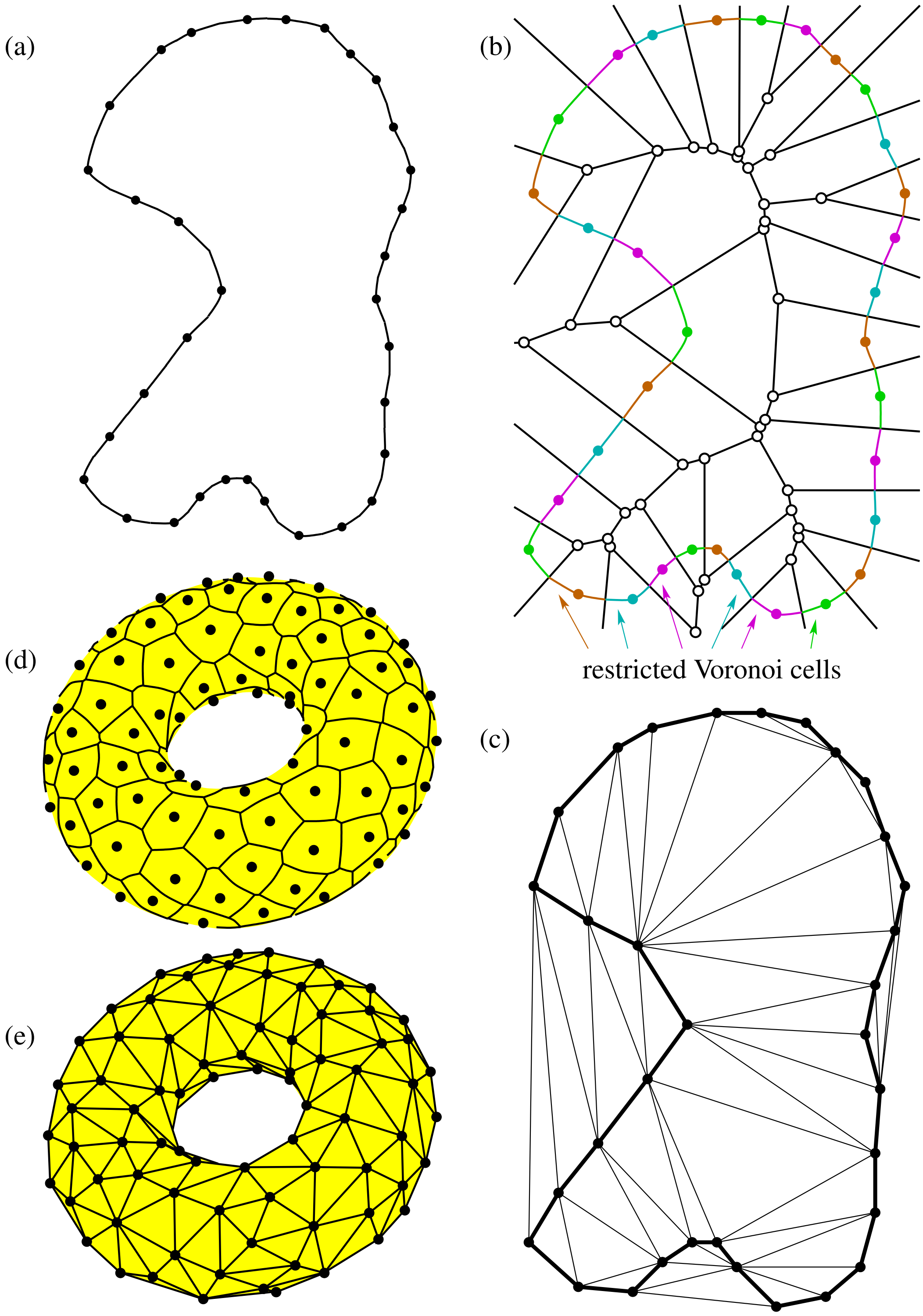

Figure 1 (a) A two-dimensional view of restricted Delaunay triangulations. The input is a smooth, closed curve Σ and a sample $V \subset \Sigma$. (b) The restricted Voronoi diagram is the restriction of the (classic) Voronoi diagram to Σ. (c) The restricted Delaunay triangulation (bold) is the dual of the restricted Voronoi diagram and a subcomplex of the (classic) Delaunay triangulation. (d) A restricted Voronoi diagram in three dimensions. (e) Its dual restricted Delaunay triangulation.

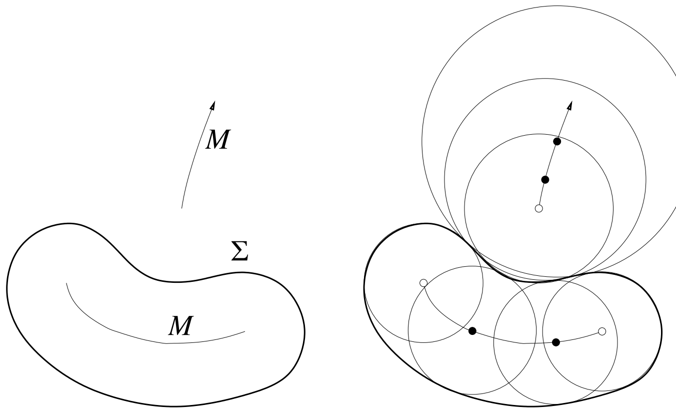

Figure 2 Left: A curve Σ and its medial axis M. Center: Some of the medial balls that define M. Balls with black centers touch two points on Σ. The white points are in the closure of the black centers. Right: A 0.5-sample of Σ (black points). The ball with center x and radius $0.5\,\mathrm{lfs}(x)$ contains a site.

A *restricted Voronoi face* is any nonempty intersection of one or more restricted Voronoi cells – i.e., $\Sigma \cap F$ for some face F in $\mathrm{Vor}\, V$. In particular, a *restricted Voronoi vertex* is the nonempty intersection of Σ with an edge in $\mathrm{Vor}\, V$; and a *restricted Voronoi edge* is the nonempty intersection of Σ with a polygonal 2-face in $\mathrm{Vor}\, V$. Typically these entities are a single point and a (curvy) path on Σ, respectively, but if V is not dense enough, they may take on more pathological forms – e.g., a restricted Voronoi "edge" could be a cycle, a pair of disjoint paths, or even a 2-dimensional blob. This paper aims to determine sampling conditions that eliminate such pathologies. The *restricted Voronoi diagram* $\mathrm{Vor}|_\Sigma V$ is the cell complex containing all the restricted Voronoi faces (including the restricted Voronoi cells).

The *Delaunay subdivision* $\mathrm{Del}\, V$ is the polyhedral complex dual to the Voronoi diagram, and the *restricted Delaunay subdivision* $\mathrm{Del}|_\Sigma V$ is the subcomplex of $\mathrm{Del}\, V$ dual to the restricted Voronoi diagram. That is, for each Voronoi face $F \in \mathrm{Vor}\, V$, let $W \subseteq V$ be the set of sites whose Voronoi cells include F and let F^* be the convex hull of W; we say that F^* is the face *dual* to F. Then $\mathrm{Del}\, V = \{F^* : F \in \mathrm{Vor}\, V\}$. The restricted Delaunay subdivision contains the dual faces whose primal faces intersect Σ; that is, $\mathrm{Del}|_\Sigma V = \{F^* \in \mathrm{Del}\, V : F \cap \Sigma \neq \emptyset\}$. The restricted Voronoi face $f = F \cap \Sigma$ has the same dual face as F, $f^* = F^*$. It is customary to subdivide the polyhedra in $\mathrm{Del}\, V$ into tetrahedra (in which case the duality is no longer strict); accordingly, we can subdivide the polygons in $\mathrm{Del}|_\Sigma V$ into triangles and call it a *restricted Delaunay triangulation*. This paper's results apply whether we do or don't.

A crucial observation in the theory of surface sampling is that the sampling density necessary for accurate approximation is proportional to a field called the *local feature size*. The *medial axis* M of Σ, illustrated in Figure 2, is the closure of the set of all points in $\mathbb{R}^3$ for which the closest point on Σ is not unique. A *medial ball* is a ball whose center lies on M and whose boundary intersects Σ (tangentially), but the interior of the ball does not. For any point $x \in \Sigma$, there are one or two medial balls that have x on their boundaries, called *medial balls at* x. One is inside Σ. If there are two, the other is outside. If not, there is an open halfspace tangent to Σ at x, disjoint from Σ, that we call a degenerate "medial ball."

The *local feature size* function is $\mathrm{lfs} : \Sigma \to \mathbb{R}$, $x \mapsto d(x, M)$ where $d(x, M) = \min_{m \in M} |xm|$. We require that Σ is smooth in the sense that $\inf_{x \in \Sigma} \mathrm{lfs}(x) > 0$. ($C^{1,1}$-continuity suffices.)

A finite point set $V \subset \Sigma$ is an *ϵ-sample of* Σ if for every point $x \in \Sigma$, there is a site $v \in V$ such that $|xv| \leq \epsilon\, \mathrm{lfs}(x)$. That is, the ball with center x and radius $\epsilon\, \mathrm{lfs}(x)$ contains at least one site. A finite $V \subset \Sigma$ is an *ϵ-Voronoi sample of* Σ if $V \neq \emptyset$ and for every site

$v \in V$ and every point $x \in \mathrm{Vor}|_\Sigma v$, $|xv| \leq \epsilon\,\mathrm{lfs}(v)$. That is, $\mathrm{Vor}|_\Sigma v$ is a subset of the ball with center v and radius $\epsilon\,\mathrm{lfs}(v)$. (Note that this condition implies the *ϵ-small condition* of Cheng et al. [18], though the converse is not true.) Only ϵ-samples are a well-known concept, but ϵ-Voronoi samples are nice because $\mathrm{lfs}(v)$ tends to give better sampling bounds than $\mathrm{lfs}(x)$.

Like the classical proofs [1, 18, 20], this paper's homeomorphism proofs rely on the Topological Ball Theorem of Edelsbrunner and Shah [23]. Given a sample $V \subset \Sigma$ of a closed surface $\Sigma \subset \mathbb{R}^3$, this theorem states that $|\mathrm{Del}|_\Sigma V|$ is homeomorphic to Σ if Σ and V satisfy two properties. The *closed ball property* is that for each Voronoi face $F \in \mathrm{Vor}\,V$, $f = F \cap \Sigma$ is either empty or a topological closed $(k-1)$-ball where k is the dimension of F. That is,

A. for a Voronoi 3-cell F, f is a topological closed disk;
B. for a Voronoi 2-face F, f is a topological closed interval or $\emptyset$;
C. for a Voronoi edge F, f contains at most one point; and
D. for a Voronoi vertex F, $f = \emptyset$.

If A–D hold, the *generic intersection property* is that for each $F \in \mathrm{Vor}\,V$, $\mathrm{int}\, f \subset \mathrm{int}\, F$ and $\mathrm{bd}\, f \subset \mathrm{bd}\, F$. In this definition, "interior" and "boundary" are interpreted by the rules of $(k-1)$-manifolds (for f) and k-manifolds (for F). (They are *not* the interior and boundary with respect to $\mathbb{R}^3$.) For a smooth Σ, the generic intersection property holds if properties A–D hold and there is no face $F \in \mathrm{Vor}\,V$ and no point $x \in F \cap \Sigma$ such that $F \subset T_x\Sigma$. That is,

E. there is no point where Σ intersects a 2-face of $\mathrm{Vor}\,V$ tangentially; and
F. there is no point where Σ intersects an edge of $\mathrm{Vor}\,V$ tangentially.

This paper is organized around proving that these conditions hold for a sufficiently dense sample V: properties A and E in Section 4, properties C and F in Section 5, and property B in Section 6. Property D ensures that $\mathrm{Del}|_\Sigma V$ contains no polyhedra – only faces of dimension two or less. Property D cannot be enforced by dense sampling, but it can be enforced by an infinitesimal perturbation of Σ so that Σ intersects no Voronoi vertex. This perturbation is easy to simulate symbolically in software simply by treating each Voronoi vertex on Σ as if it were strictly inside Σ (when deciding which faces of $\mathrm{Del}\,V$ are in $\mathrm{Del}|_\Sigma V$).

Unlike in Dey [20] or Cheng et al. [18], our proof of property A does not rely on property B or C. Property A holds for a 0.4401-sample or a 0.7861-Voronoi sample, whereas we prove property B only for a 0.3245-sample or a 0.4132-Voronoi sample. Property B (restricted Voronoi edges) is the bottleneck that determines our sampling requirements.

Some algorithms for triangulating surfaces guarantee topological correctness without RDTs, by other methods [4, 8, 19, 27, 29]. One alternative is to consider Voronoi diagrams with other distance metrics. Dyer, Zhang, and Möller [21, 22] and others [28, 7] use intrinsic distances within Σ, also known as geodesic distances when Σ is smooth, to define *intrinsic Voronoi diagrams* that dualize to *intrinsic Delaunay triangulations* (IDTs). Advantages are that the Voronoi cells are trivially star-shaped, and the sampling requirements needed to guarantee a homeomorphic triangulation are mild [22]. But intrinsic distances on smooth surfaces are painful to compute [30]. Restricted Delaunay triangulations will probably remain popular as an easy alternative. So let us see how far we can push them.

3 A relationship between surface points and nearby tangent planes

For a smooth, closed surface Σ and a point $x \in \Sigma$, let $T_x\Sigma \subset \mathbb{R}^3$ denote the plane tangent to Σ at x. ($T_x\Sigma$ passes through x; not necessarily through the origin.) Lemma 1, below, establishes a relationship between $T_x\Sigma$ and v for two nearby points $v, x \in \Sigma$. This relationship prepares us to prove in Section 4 that under suitable sampling conditions, a restricted Voronoi cell is a topological disk with a star-shaped projection on its site's tangent plane. Lemma 1 is surprisingly strong; the constant ξ (as it is applied in Theorem 6) will likely be hard to beat.

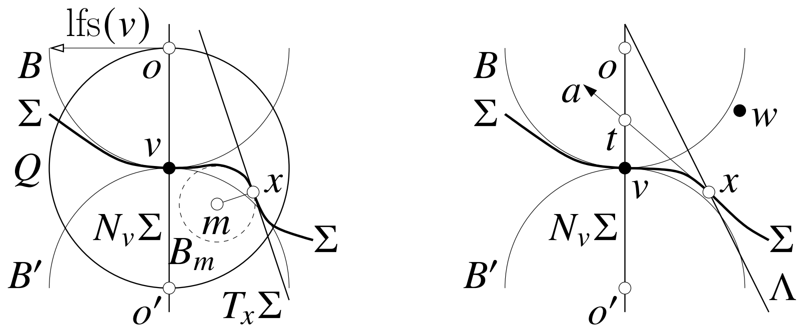

Figure 3 Left: for two nearby points $v, x \in \Sigma$, suppose that the tangent plane $T_x\Sigma$ does not intersect oo', as shown. This leads to a contradiction; hence $T_x\Sigma$ must intersect oo'. The medial ball B_m is tangent to Σ at x. The center m of B_m cannot lie in the open ball Q. The points v, x, o, and o' lie on the plane of the page, but m and w generally do not; imagine m floating above the page. The dashed circle shows the page's cross section of B_m, but B_m is larger. The surface Σ cannot intersect the open balls B, B', and B_m, so B and B_m are disjoint. Right: the plane Λ bisects vw. The ray $a \in T_x\Sigma$ intersects the relative interior of oo' and is strictly on the same side of Λ as v.

Let B and B' be the two open balls of radius $\operatorname{lfs}(v)$ tangent to Σ at v, and let o and o' be their centers. As B and B' are subsets of the open medial balls at v, they are disjoint from Σ.

▶ **Lemma 1.** *Consider two points $v, x \in \Sigma$ such that $|vx| < \xi \operatorname{lfs}(v)$, where $\xi = \sqrt{(\sqrt{5}-1)/2} \doteq 0.786151$. Then o and o' lie on strictly opposite sides of $T_x\Sigma$.*

Proof. Suppose for the sake of contradiction that o and o' do not lie on strictly opposite sides of $T_x\Sigma$, as illustrated in Figure 3, left. Then $T_x\Sigma \neq T_v\Sigma$ and $x \neq v$. Moreover, either $oo' \subset T_x\Sigma$ or $T_x\Sigma$ does not intersect the relative interior of oo'.

Let B_m be the open medial ball tangent to Σ at x that is on the same side of $T_x\Sigma$ as v (either side if $v \in T_x\Sigma$), as illustrated. If B_m is an open halfspace then $T_x\Sigma = \text{boundary } B_m$, $v \in T_x\Sigma$ (as $v \notin B_m$), $T_v\Sigma = T_x\Sigma$ (as $\Sigma \cap B_m = \emptyset$), and the lemma follows. So assume B_m is bounded. Its center m lies on Σ's medial axis. The line segment xm is perpendicular to $T_x\Sigma$.

Observe that v is in the relative interior of oo'. If $oo' \subset T_x\Sigma$, then $\angle vxm = \angle oxm = \angle o'xm = 90°$. Otherwise, $T_x\Sigma$ does not intersect the relative interior of oo', so $\angle vxm < 90°$, $\angle oxm \leq 90°$, and $\angle o'xm \leq 90°$ (the last two because o and o' cannot be on the side of $T_x\Sigma$ opposite from v). By Pythagoras' Theorem, $|ox|^2 + |mx|^2 \geq |om|^2$ and $|vx|^2 + |mx|^2 \geq |vm|^2$. As m lies on the medial axis, $|vm| \geq \operatorname{lfs}(v)$ (by the definition of lfs), so $|vx|^2 + |mx|^2 \geq \operatorname{lfs}(v)^2$.

The surface Σ intersects none of the open balls B, B', or B_m, but it passes between B and B' at v. As Σ is closed and cuts space into two pieces, one containing B and one containing B', the ball B_m must lie in one of those two pieces. Choose the labels B and B' so that B_m lies in the same piece as B', as illustrated; then B_m must be disjoint from B. The radii of B and B_m are $\operatorname{lfs}(v)$ and $|mx|$ respectively, so $|om| \geq \operatorname{lfs}(v) + |mx|$. Combining this with the inequality $|ox|^2 + |mx|^2 \geq |om|^2$ gives $|ox|^2 \geq \operatorname{lfs}(v)^2 + 2\operatorname{lfs}(v)\,|mx|$. Combining this with the inequality $|mx|^2 \geq \operatorname{lfs}(v)^2 - |vx|^2$ gives $|ox|^2 \geq \operatorname{lfs}(v)^2 + 2\operatorname{lfs}(v)\sqrt{\operatorname{lfs}(v)^2 - |vx|^2}$.

Let $N_v\Sigma$ be the line through o', v, and o (the vertical axis in Figure 3). Create a coordinate system with $v = (0,0,0)$ and $x = (x_h, x_v, 0)$ such that x_v is the coordinate in the direction parallel to $N_v\Sigma$ and x_h is the distance from $N_v\Sigma$ to x (the horizontal axis in Figure 3). Then $|ox|^2 + |o'x|^2 = x_h^2 + (x_v - \operatorname{lfs}(v))^2 + x_h^2 + (x_v + \operatorname{lfs}(v))^2 = 2x_h^2 + 2x_v^2 + 2\operatorname{lfs}(v)^2 = 2\,|vx|^2 + 2\operatorname{lfs}(v)^2$. Rewrite this as $|vx|^2 = (|ox|^2 + |o'x|^2 - 2\operatorname{lfs}(v)^2)/2$. As $x \notin B'$, $|o'x|^2 \geq \operatorname{lfs}(v)^2$. Combining these with the inequality $|ox|^2 \geq \operatorname{lfs}(v)^2 + 2\operatorname{lfs}(v)\sqrt{\operatorname{lfs}(v)^2 - |vx|^2}$ gives $|vx|^2 \geq \operatorname{lfs}(v)\sqrt{\operatorname{lfs}(v)^2 - |vx|^2}$.

As $|vx| < \xi \operatorname{lfs}(v)$, we have $\xi^2 > |vx|^2/\operatorname{lfs}(v)^2 \geq \sqrt{1 - |vx|^2/\operatorname{lfs}(v)^2} > \sqrt{1-\xi^2}$, which is equivalent to $\xi^4 + \xi^2 - 1 > 0$, hence $\xi > \sqrt{(\sqrt{5}-1)/2}$. The result follows by contradiction. ◀

4 Restricted Voronoi cells are topological disks

This section investigates sampling conditions that guarantee that (1) every restricted Voronoi cell has the topology of a closed disk (closed ball property A), (2) the projection of each restricted Voronoi cell onto its site's tangent plane is star-shaped, and (3) no 2-face in Vor V intersects Σ tangentially (generic intersection property E). Theorem 6 shows that a 0.78-Voronoi sample suffices, and Corollary 9 shows that a 0.44-sample suffices.

Consider a site $v \in V$, its Voronoi cell Vor v, and its restricted Voronoi cell $\mathrm{Vor}|_\Sigma v = \Sigma \cap \mathrm{Vor}\, v$. Let φ be the map that orthogonally projects $\mathbb{R}^3$ onto $T_v\Sigma$. Note that $\varphi(v) = v$.

Define a *radial path* to be a topological closed interval $\gamma \subset \mathrm{Vor}|_\Sigma v$ such that

1. one endpoint of γ is the site v,
2. the other endpoint – call it z – lies on the boundary of Vor v,
3. every point on $\gamma \setminus \{z\}$ lies in the interior of Vor v, and
4. $\varphi|_\gamma$ is a homeomorphism from γ to a line segment on $T_v\Sigma$ with endpoints v and $\varphi(z)$, where $\varphi|_\gamma$ denotes the restriction of φ to the domain γ.

We will see that under suitable sampling conditions, every point in $\mathrm{Vor}|_\Sigma v$ lies on exactly one radial path, except v itself (Lemma 4). It follows that we can decompose $\mathrm{Vor}|_\Sigma v$ into radial paths such that no two share a point besides v (Lemma 5). That is, if we remove v from each radial path, then we have a partition of $\mathrm{Vor}|_\Sigma v \setminus \{v\}$ into paths. Therefore, $\varphi(\mathrm{Vor}|_\Sigma v)$ is star-shaped. Although $\mathrm{Vor}|_\Sigma v$ itself is not star-shaped, its decomposition into radial paths is a curvy variant of "star-shaped." As the lengths of the projected radial paths vary continuously with their polar angles, $\mathrm{Vor}|_\Sigma v$ is homeomorphic to a closed disk (Theorem 6).

Let $N_v\Sigma$ be the line normal to Σ at v (orthogonal to $T_v\Sigma$). Let B and B' be the two open balls of radius $\mathrm{lfs}(v)$ tangent to Σ at v, and let o and o' be their centers. Then $o, o' \in N_v\Sigma$.

The following lemma implies that if you are standing on the boundary of $\mathrm{Vor}|_\Sigma v$ and you walk toward v on a radial path, you immediately enter the interior of Vor v. (The proof of Lemma 4 develops this idea further.) It also implies generic intersection property E.

▶ **Lemma 2.** *Consider two distinct sites $v, w \in V$ and a point $x \in \mathrm{Vor}|_\Sigma v \cap \mathrm{Vor}|_\Sigma w$. Suppose that $|vx| < \xi\,\mathrm{lfs}(v)$ where $\xi = \sqrt{(\sqrt{5}-1)/2} \doteq 0.786151$. Let Λ be the plane that orthogonally bisects the line segment vw (thus $x \in \Lambda$). By Lemma 1, $T_x\Sigma$ intersects the relative interior of the line segment oo' at a lone point t. Let a be the open ray $\vec{xt}$, and observe that $a \subset T_x\Sigma$.*

Then v and a are strictly on the same side of Λ.

Proof. See Figure 3, right. Neither B nor B' intersects Σ, hence neither ball contains w, hence $|vo| \leq |wo|$ and $|vo'| \leq |wo'|$. Therefore, each of o and o' lies either on Λ or on the same side of Λ as v, as illustrated. (More broadly, $oo' \subset \mathrm{Vor}\, v$.) As $v \in oo'$ and $v \notin \Lambda$, Λ does not intersect the relative interior of oo'. By contrast, a does intersect the relative interior of oo' (at t). Recall that a's origin x lies on Λ. Therefore, the open ray a is strictly on the same side of Λ as the relative interior of oo', which contains v. ◀

Lemma 4, below, shows that under suitable sampling conditions, every point in $\mathrm{Vor}|_\Sigma v \setminus \{v\}$ lies on one and only one radial path. It depends on the simple observation of Lemma 3.

▶ **Lemma 3.** *Let $v, x \in \Sigma$ be two points such that $|vx| < \xi\,\mathrm{lfs}(v)$. There exists an open neighborhood $N \subset \Sigma$ of x such that $\varphi|_N$ is a homeomorphism from N to its image $\varphi(N) \subset T_v\Sigma$.*

Proof. As $|vx| < \xi\,\mathrm{lfs}(v)$, by Lemma 1 (or Lemma 13), $T_x\Sigma$ is not perpendicular to $T_v\Sigma$. It follows from the smoothness of Σ that if N is sufficiently small, $\varphi|_N$ is injective. As $\varphi|_N$ is injective and both $\varphi|_N$ and its inverse are continuous, $\varphi|_N$ is a homeomorphism. ◀

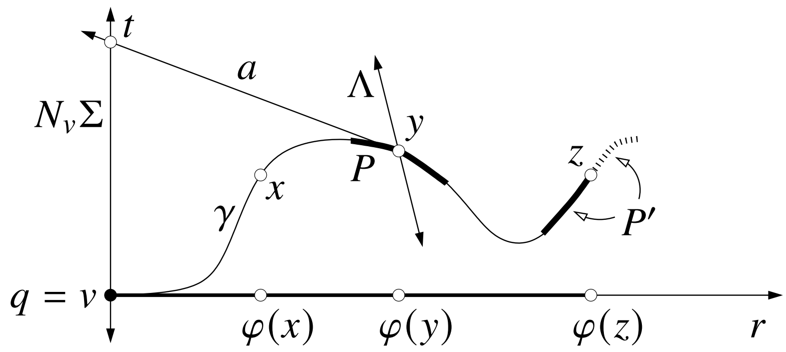

Figure 4 A radial path γ with endpoints v and z. (The path P' extends past γ on Σ.)

▶ **Lemma 4.** *Consider a site $v \in V$, its restricted Voronoi cell $C = \mathrm{Vor}|_\Sigma v$, and a point $x \in C \setminus \{v\}$. Let $r \in T_v\Sigma$ be the closed ray with origin v that passes through $\varphi(x)$. Suppose that for every point $y \in C$, $|vy| < \xi\,\mathrm{lfs}(v)$, where $\xi = \sqrt{(\sqrt{5}-1)/2} \doteq 0.786151$.*

Then there is a unique radial path $\gamma \subset C$ such that $x \in \gamma$. Furthermore, γ is the only radial path such that $\varphi(\gamma) \subseteq r$.

Proof. For every point $y \in C \setminus \{v\}$ (including x), $\varphi(y) \neq v$, as if $\varphi(y) = v$ we have a contradiction: $|vy| < \xi\,\mathrm{lfs}(v)$ and $y \neq v$ imply that y is in B or B' and thus not in C.

Define the point set $\varphi|_C^{-1}(r) = \{y \in C : \varphi(y) \in r\}$ (the intersection of C with the closed halfplane with boundary $N_v\Sigma$, passing through x). Clearly, $x \in \varphi|_C^{-1}(r)$. Let γ be the connected component of $\varphi|_C^{-1}(r)$ that contains x. We will show that γ is a radial path.

As $\gamma \subset C$, for every point $y \in \gamma$, $|vy| < \xi\,\mathrm{lfs}(v)$ and by Lemma 3 there exists an open neighborhood $N \subset \Sigma$ of y such that $\varphi|_N$ is a homeomorphism, so $\varphi|_{N\cap\gamma}$ is a homeomorphism from $N \cap \gamma$ to its image $\varphi(N \cap \gamma)$. In other words, $\varphi|_\gamma$ is a local homeomorphism from γ to its image $\varphi(\gamma)$. As γ is connected and $\varphi(\gamma)$ is embedded in the ray r, $\varphi|_\gamma$ is a (global) homeomorphism. (Intuitively, the map φ cannot cause the path to double back on itself, so $\varphi|_\gamma$ is an injection.) Therefore, γ is a topological interval or a lone point.

As C is compact and r is closed, $\varphi|_C^{-1}(r)$ is compact and γ is compact. Let q and z be the endpoints of γ, chosen so that $|v\varphi(q)| \leq |v\varphi(z)|$; see Figure 4. As $\varphi|_\gamma$ is a homeomorphism, $\varphi(q)$ and $\varphi(z)$ are the endpoints of $\varphi(\gamma)$. As $\varphi(\gamma)$ contains $\varphi(x)$ and $\varphi(x) \neq v$, $\varphi(z) \neq v$ and $z \neq v$. We will show that $q = v$ (which implies that $\varphi(C)$ is star-shaped) and that z is on the boundary of $\mathrm{Vor}\, v$, thereby establishing the first two criteria for γ to be a radial path.

But first, we show that $\gamma \setminus \{z\}$ is in the interior of $\mathrm{Vor}\, v$, the third criterion for γ to be a radial path. Suppose for the sake of contradiction that a point $y \in \gamma \setminus \{z\}$ lies on the boundary of $\mathrm{Vor}\, v$. Then y also lies in the restricted Voronoi cell $\mathrm{Vor}|_\Sigma w$ of another site $w \in V \setminus \{v\}$, and $y \in \Lambda$ where Λ is the plane that orthogonally bisects vw. Clearly, $y \neq v$. By Lemma 1, $T_y\Sigma$ intersects $N_v\Sigma$ at a lone point t. Let a be the open ray $\vec{yt}$. Observe that $a \subset T_y\Sigma$; moreover, a is tangent to γ at y, as illustrated in Figure 4.

By Lemma 2, v and a are strictly on the same side of Λ. Hence if you walk along γ from y to z – opposite to the direction of a – you enter w's side of Λ at the instant you leave y, as illustrated. This contradicts the fact that $\gamma \in \mathrm{Vor}|_\Sigma v$. So $\gamma \setminus \{z\}$ is in the interior of $\mathrm{Vor}\, v$.

Let us return to the first two criteria for γ to be a radial path. Consider a point $y \in \gamma \setminus \{v\}$. By Lemma 3, there exists an open neighborhood $N \subset \Sigma$ of y such that $\varphi|_N$ is a homeomorphism. Define $\varphi|_N^{-1}(r) = \{p \in N : \varphi(p) \in r\}$ and let P be the connected component of $\varphi|_N^{-1}(r)$ that contains y, illustrated in Figure 4. As $\varphi(y)$ is in the interiors of r and $\varphi(N)$, $\varphi(y)$ is in the interior of $r \cap \varphi(N)$. As $\varphi|_N$ is a homeomorphism, y is in the relative interior of $\varphi|_N^{-1}(r)$, so P is a path (topological interval) on Σ with y in its relative interior.

First, consider the case where y is in the interior of $\mathrm{Vor}\, v$ (but $y \neq v$). Then we can shrink the open neighborhood N of y so that $N \subset \mathrm{Vor}\, v$ and thus $N \subset C$, and thereby have $\varphi|_N^{-1}(r) \subseteq \varphi|_C^{-1}(r)$. As γ is the connected component of $\varphi|_C^{-1}(r)$ that contains y, $P \subseteq \gamma$. Hence y is not an endpoint of γ. We have seen that $\gamma \setminus \{z\}$ is in the interior of $\mathrm{Vor}\, v$; it follows that only v and z can be endpoints of γ. That is, the endpoint q is either v or z. Moreover, as $z \neq v$ is an endpoint of γ, z is on the boundary of $\mathrm{Vor}\, v$ (establishing the second criterion).

Second, consider the case where $y = z$. In this case, the path P looks like P' in Figure 4. We use this case to show that $q \neq z$. Suppose for the sake of contradiction that $q = z$; then $\gamma = \{z\}$. It follows that as you walk along P from z, you exit the restricted Voronoi cell C in both directions along P. Let a be the open ray $\vec{zt}$ where $\{t\} = T_z\Sigma \cap N_v\Sigma$ (hence $a \subset T_z\Sigma$); a is tangent to P at z. As P exits C, there exists a site $w \in V \setminus \{v\}$ and a plane Λ that orthogonally bisects vw such that $z \in \Lambda$ and a enters w's side of Λ at z. But this contradicts the fact that, by Lemma 2, v and a are strictly on the same side of Λ. Thus $q \neq z$, so $q = v$.

Therefore, the endpoints of γ are v and z, z is on the boundary of $\mathrm{Vor}\, v$, $\gamma \setminus \{z\}$ is in its interior, and $\varphi|_\gamma$ is a homeomorphism from γ to $v\varphi(z)$. By definition, γ is a radial path.

To see that γ is the *only* radial path containing x, observe that every radial path containing x is a subset of $\varphi|_C^{-1}(r)$, and moreover is a subset of γ (because a radial path is connected). No strict subset of γ can be a radial path, because every connected strict subset of γ is missing either v or a point on the boundary of $\mathrm{Vor}\, v$.

The reasoning of this proof holds equally well if we replace x with any other point $x' \in \varphi|_C^{-1}(r) \setminus \{v\}$, so every connected component of $\varphi|_C^{-1}(r)$ contains v. Therefore, $\varphi|_C^{-1}(r)$ is connected. Hence $\gamma = \varphi|_C^{-1}(r)$ and no radial path besides γ has its projection on r. ◀

It follows that we can decompose $\mathrm{Vor}|_\Sigma v$ into radial paths. Hence $\varphi(\mathrm{Vor}|_\Sigma v)$ is star-shaped. It also follows that the orthogonal projection φ, restricted to $\mathrm{Vor}|_\Sigma v$, is a homeomorphism.

▶ **Lemma 5.** *Let $v \in V$ be a site and let $C = \mathrm{Vor}|_\Sigma v$ be its restricted Voronoi cell. Suppose that for every point $y \in C$, $|vy| < \xi\, \mathrm{lfs}(v)$, where $\xi = \sqrt{(\sqrt{5} - 1)/2} \doteq 0.786151$.*

Let Γ be the set of all radial paths for all points in $C \setminus \{v\}$.

Then $\bigcup_{\gamma \in \Gamma} \gamma = C$; hence $\varphi(C)$ is star-shaped. Moreover, no two paths in Γ share a common point besides v, and there is a one-to-one correspondence between paths in Γ and points where Σ intersects the boundary of $\mathrm{Vor}\, v$.

Moreover, $\varphi|_C$ is a homeomorphism from C to its image $\varphi(C)$ on $T_v\Sigma$.

Proof. By Lemma 4, for each point $x \in C \setminus \{v\}$, there is a unique radial path $\gamma \subset C$ such that $x \in \gamma$. Every radial path contains v. Hence $\bigcup_{\gamma \in \Gamma} \gamma = C$. As each $x \in C \setminus \{v\}$ lies on only one radial path, no two paths in Γ share a common point besides v. By definition, each radial path contains exactly one point on the boundary of $\mathrm{Vor}\, v$. Hence there is a one-to-one correspondence between radial paths and points where Σ intersects the boundary of $\mathrm{Vor}\, v$.

Let us see that $\varphi|_C$ is an injection. Consider two points $x, y \in C$ such that $\varphi(x) = \varphi(y)$; we will see that $x = y$. For every radial path $\gamma \in \Gamma$, $\varphi|_\gamma$ is a homeomorphism by the definition of radial path, so if x and y lie on the same radial path, then $x = y$. If x and y lie on distinct radial paths, then $x = y = v$, because by Lemma 4, for any two distinct radial paths $\gamma_1, \gamma_2 \in \Gamma$, $\varphi(\gamma_1)$ and $\varphi(\gamma_2)$ lie on two distinct rays with origin v.

As C is compact and $\varphi|_C$ is injective and continuous, $\varphi|_C$ is a homeomorphism [33]. ◀

Lemma 5 shows that $\mathrm{Vor}|_\Sigma v$ is homeomorphic to its image $I_v = \varphi(\mathrm{Vor}|_\Sigma v)$ on $T_v\Sigma$, but what is the shape of I_v? We obtain a homeomorphism from I_v to a closed unit disk on $T_v\Sigma$ by simply scaling each line segment $\varphi(\gamma)$ to have unit length. Thus we arrive at this section's main theorem, Theorem 6, which states that $\mathrm{Vor}|_\Sigma v$ is a topological closed disk. The proof is deferred to the full-length paper [32], but here is a sketch of the ideas.

Let $E = \{\varphi(\gamma) : \gamma \in \Gamma\}$ be the set of the orthogonal projections of the radial paths onto $T_v\Sigma$. Then we can write $I_v = \bigcup_{e \in E} e$, a decomposition of I_v into line segments with endpoint v, no two leaving v in the same direction (but every direction on $T_v\Sigma$ is represented).

For every point $x \in I_v \setminus \{v\}$, let $l(x)$ be the length of the unique line segment in E that contains x. Thus l is a function over the domain $I_v \setminus \{v\}$, but $l(v)$ is not defined. One can show that l is continuous [32]. This is a consequence of two facts: I_v is a compact point set and every point on a line segment $e \in E$ except one endpoint is in the interior of I_v.

Let $\chi : I_v \to T_v\Sigma$ map each line segment in E to a line segment with unit length (while preserving its direction) – specifically, $\chi(x) = v + \frac{1}{l(x)}(x - v)$ for $x \neq v$ and $\chi(v) = v$. Then χ is continuous as l is continuous and positive. As χ is a bijective, continuous map with a continuous inverse, χ is a homeomorphism from I_v to a closed unit disk.

▶ **Theorem 6.** *Let $v \in V$ be a site and let $C = \mathrm{Vor}|_\Sigma v$ be its restricted Voronoi cell. Suppose that for every point $y \in \mathrm{Vor}|_\Sigma v$, $|vy| < \xi\,\mathrm{lfs}(v)$, where $\xi = \sqrt{(\sqrt{5}-1)/2} \doteq 0.786151$.*

Then $\chi \circ \varphi|_C$ is a homeomorphism from $\mathrm{Vor}|_\Sigma v$ to a closed unit disk on $T_v\Sigma$.

If we impose the condition of Theorem 6 on *all* the restricted Voronoi cells, every connected component of Σ has at least six sites on it. Lemma 7 follows easily from Lemmas 4 and 13, but there isn't quite enough space here for the proof; see the full-length paper [32].

▶ **Lemma 7.** *Let V be an ϵ-Voronoi sample of Σ for some $\epsilon < \xi = \sqrt{(\sqrt{5}-1)/2} \doteq 0.786151$. Every connected component of Σ has at least six sites and six restricted Voronoi cells on it.*

To apply Theorem 6 to ϵ-samples, observe that 0.44-samples are 0.786-Voronoi samples.

▶ **Lemma 8** (Feature Translation Lemma [3, 20]). *Let $\Sigma \subset \mathbb{R}^3$ be a smooth, closed surface and let $p, q \in \Sigma$ be points such that $|pq| \leq \epsilon\,\mathrm{lfs}(p)$ for some $\epsilon < 1$. Then*

$$\mathrm{lfs}(p) \leq \frac{1}{1-\epsilon}\mathrm{lfs}(q) \quad \textit{and} \quad |pq| \leq \frac{\epsilon}{1-\epsilon}\mathrm{lfs}(q).$$

▶ **Corollary 9.** *Let V be an ϵ-sample of Σ for $\epsilon < \frac{\xi}{\xi+1} \doteq 0.440137$.*

Then every restricted Voronoi cell in $\mathrm{Vor}|_\Sigma V$ is homeomorphic to a closed disk (closed disk property A), Σ does not intersect any 2-face of $\mathrm{Vor}\,V$ tangentially (generic intersection property E), every connected component of Σ has at least six sites and six restricted Voronoi cells on it, and no restricted Voronoi cell intersects the interior of another.

Proof. Consider any site $v \in V$ and any point $x \in \mathrm{Vor}|_\Sigma v$. As V is an ϵ-sample, $|vx| \leq \epsilon\,\mathrm{lfs}(x)$. By the Feature Translation Lemma (Lemma 8), $|vx| \leq \frac{\epsilon}{1-\epsilon}\,\mathrm{lfs}(v) < \xi\,\mathrm{lfs}(v)$.

The first three claims follow from Theorem 6 and Lemmas 2 and 7, respectively. The final claim follows from Lemma 5 because every point in the interior of $\mathrm{Vor}|_\Sigma v$ is in the interior of $\mathrm{Vor}\,v$ (by the definition of radial path) and cannot be shared with another cell. ◀

5 Restricted Voronoi vertices are lone points

A restricted Voronoi vertex is a nonempty intersection of Σ with an edge in $\mathrm{Vor}\,V$. However, without suitable sampling conditions, such an intersection might contain many points, even infinitely many. This section describes sampling conditions that guarantee closed ball property C: an intersection of three distinct restricted Voronoi cells contains at most one point, thereby justifying the name "vertex." Generic intersection property F comes as a byproduct. Lemma 10 shows that a 0.49-Voronoi sample suffices, and Corollary 11 shows that a 0.33-sample suffices (which follows from Lemmas 10 and 8). Both proofs are postponed to the full-length paper [32], as restricted Voronoi vertices are not the bottleneck limiting our homeomorphism theorems' sample bounds. (Restricted Voronoi edges are the bottleneck; see Section 6.) Note that Cheng et al. [18] prove Lemma 10 for a 0.15-Voronoi sample.

▶ **Lemma 10.** *Consider three distinct sites $v, v', v'' \in V$ and the triangle $\tau = \triangle vv'v''$, where v is the vertex at τ's largest plane angle. Let $f = \mathrm{Vor}|_\Sigma v \cap \mathrm{Vor}|_\Sigma v' \cap \mathrm{Vor}|_\Sigma v''$, the restricted Voronoi face dual to τ. Let $\ell_\tau \subset \mathbb{R}^3$ be the line containing all points equidistant to the sites v, v', and v'' (thus $f \subset \ell_\tau$). Suppose that for every point $y \in f$, $|vy| < \kappa\,\mathrm{lfs}(v)$, where κ is the positive real root of $\kappa^4 = 4(1-\kappa^2)(1-\sqrt{3}\kappa)^2$, with approximate value $\kappa \doteq 0.495683$.*

Then f contains at most one point (i.e., a restricted Voronoi vertex). Moreover, if f contains a point, Σ is not tangent to ℓ_τ at that point.

▶ **Corollary 11.** *Let V be an ϵ-sample of Σ for $\epsilon < \frac{\kappa}{\kappa+1} \doteq 0.331409$. Consider three distinct sites $v, v', v'' \in V$ and let $f = \mathrm{Vor}|_\Sigma v \cap \mathrm{Vor}|_\Sigma v' \cap \mathrm{Vor}|_\Sigma v''$. Let $\ell_\tau \subset \mathbb{R}^3$ be the line containing all points equidistant to the sites v, v', and v''.*

Then f contains at most one point, and Σ is not tangent to ℓ_τ at that point.

6 Restricted Voronoi edges are topological intervals

Theorem 6 and Corollary 9 give conditions under which restricted Voronoi cells are topological closed disks. Lemma 10 and Corollary 11 give conditions under which the intersection of three distinct restricted Voronoi cells is at most one point. What about an intersection of two distinct restricted Voronoi cells? That could be empty, a restricted Voronoi vertex, or a *restricted Voronoi edge*, the last being a nonempty intersection of Σ with a 2-face of $\mathrm{Vor}\,V$. Under suitable sampling conditions, Lemma 17, below, guarantees closed ball property B: each restricted Voronoi edge is a topological interval.

The next six lemmas derive conditions in which an intersection $\mathrm{Vor}|_\Sigma v \cap \mathrm{Vor}|_\Sigma w$ is one interval or one isolated point. Lemma 15 applies to 0.32-samples, whereas Lemma 16 applies to 0.41-Voronoi samples, and Lemma 17 concludes both. Lemma 12 has no sampling requirements, only topological requirements; see the full-length paper for a proof [32].

▶ **Lemma 12.** *Let $\mathrm{Vor}|_\Sigma V$ be a restricted Voronoi diagram. Suppose that every restricted Voronoi cell is a topological closed disk and every intersection of three distinct restricted Voronoi cells is either empty or a lone point (henceforth called a restricted Voronoi vertex). Suppose also that no restricted Voronoi cell intersects the interior of another.*

Then for every pair of distinct sites $v, w \in V$, $\mathrm{Vor}|_\Sigma v \cap \mathrm{Vor}|_\Sigma w$ is one of these three: empty; a topological circle containing no restricted Voronoi vertex; or a union of disjoint topological closed intervals and isolated points, where each isolated point is a restricted Voronoi vertex and each interval contains exactly two restricted Voronoi vertices which are its endpoints.

Moreover, if each connected component of Σ has at least three sites in V lying on it, then the possibility that $\mathrm{Vor}|_\Sigma v \cap \mathrm{Vor}|_\Sigma w$ is a topological circle is eliminated, every restricted Voronoi cell has at least two restricted Voronoi vertices on its boundary, and every connected component of Σ has at least two restricted Voronoi vertices on it.

A closed Σ cuts space into two pieces, a bounded *inside* piece and an unbounded *outside* piece. For a point $x \in \Sigma$, let n_x denote the outside-facing vector normal to Σ at x (and normal to $T_x\Sigma$). Let $\angle(n_p, n_q) \in [0°, 180°]$ denote the angle separating two vectors.

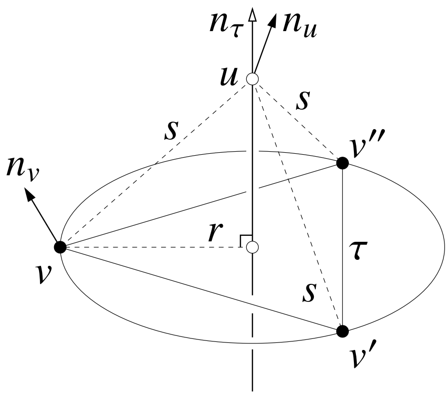

Figure 5 The sites v, v', and v'' and the restricted Voronoi vertex u lie on Σ (not shown).

▶ **Lemma 13** (Normal Variation Lemma [25]). *Consider two points $p, q \in \Sigma$ and let $\delta = |pq|/\mathrm{lfs}(p)$. If $\delta < \sqrt{4\sqrt{5}-8} \doteq 0.971736$, then $\angle(n_p, n_q) \le \eta(\delta)$ where*

$$\eta(\delta) = \arccos\left(1 - \frac{\delta^2}{2\sqrt{1-\delta^2}}\right) \approx \delta + \frac{7}{24}\delta^3 + O(\delta^5) \text{ radians.}$$

▶ **Lemma 14** (Triangle Normal Lemma [25]). *Let τ be a triangle whose vertices lie on Σ. Let r be the radius of τ's circumscribing circle. Let v be a vertex of τ and let ϕ be τ's plane angle at v. Let n_τ be a vector normal to τ. Let $\mathrm{aff}\,\tau$ denote the affine hull of τ. Then*

$$\sin\angle(n_\tau, n_v) = \sin\angle(\mathrm{aff}\,\tau, T_v\Sigma) \le \frac{r}{\mathrm{lfs}(v)} \max\left\{\cot\frac{\phi}{2}, 1\right\}.$$

▶ **Lemma 15.** *Let u be a restricted Voronoi vertex and let $\tau = \triangle vv'v''$ be its dual restricted Delaunay triangle. (If u's dual face is a polygon, you may choose any three of its vertices.) Let n_τ be a vector normal to τ, directed so that $\angle(n_v, n_\tau) \le 90°$ (as illustrated in Figure 5). Let $s = |vu| = |v'u| = |v''u|$ and suppose that $s \le 0.3245\,\mathrm{lfs}(u)$.*

Then $\angle(n_u, n_\tau) < 90°$ and $\angle(n_v, n_\tau) < 90°$. Equivalently, $n_u \cdot n_\tau$ and $n_v \cdot n_\tau$ are positive.

Proof. Let $w \in \{v, v', v''\}$ be the vertex at τ's largest plane angle. As $|vu| = |wu| = s \le 0.3245\,\mathrm{lfs}(u)$, by the Normal Variation Lemma (Lemma 13), $\angle(n_v, n_u) \le \eta(0.3245) < 19.21°$ and $\angle(n_w, n_u) \le \eta(0.3245) < 19.21°$.

Let r be τ's circumradius. As Figure 5 illustrates, $r \le s$, because u lies on the line perpendicular to τ through τ's circumcenter and r is the distance from v to that line. By the Feature Translation Lemma (Lemma 8), $\mathrm{lfs}(u) \le \mathrm{lfs}(v)/(1 - 0.3245)$ and $\mathrm{lfs}(u) \le \mathrm{lfs}(w)/(1-0.3245)$. Hence $r \le s \le 0.3245\,\mathrm{lfs}(u) \le \frac{0.3245}{0.6755}\,\mathrm{lfs}(v)$ and $r \le \frac{0.3245}{0.6755}\,\mathrm{lfs}(w)$.

If τ's plane angle at v is $53.932°$ or greater, then by the Triangle Normal Lemma (Lemma 14), $\sin\angle(n_v, n_\tau) \le r \cot 26.966°/\mathrm{lfs}(v) < (0.3245/0.6755) \cdot 1.9655 < 0.9442$. Therefore, $\angle(n_v, n_\tau) < 70.77°$ and $\angle(n_u, n_\tau) \le \angle(n_v, n_u) + \angle(n_v, n_\tau) < 19.21° + 70.77° = 89.98°$.

Otherwise, τ's plane angle at v is less than $53.932°$, so τ's largest plane angle (at w) is greater than $(180° - 53.932°)/2 = 63.034°$. By the Triangle Normal Lemma, $\sin\angle(n_w, n_\tau) \le r \cot 31.517°/\mathrm{lfs}(w) < (0.3245/0.6755) \cdot 1.6308 < 0.78342$. Therefore, either $\angle(n_w, n_\tau) < 51.575°$ or $\angle(n_w, n_\tau) > 128.425°$. The latter case is not possible, because $\angle(n_w, n_\tau) \le \angle(n_w, n_u) + \angle(n_u, n_v) + \angle(n_v, n_\tau) < 19.21° + 19.21° + 90° = 128.42°$. In the former case, $\angle(n_u, n_\tau) \le \angle(n_w, n_u) + \angle(n_w, n_\tau) < 19.21° + 51.575° = 70.785°$ and $\angle(n_v, n_\tau) \le \angle(n_v, n_u) + \angle(n_w, n_u) + \angle(n_w, n_\tau) < 19.21° + 19.21° + 51.575° = 89.995°$. ◀

▶ **Lemma 16.** *Let u be a restricted Voronoi vertex and let $\tau = \triangle vv'v''$ be its dual restricted Delaunay triangle. (If u's dual face is a polygon, you may choose any three of its vertices.) Let $w \in \{v, v', v''\}$ be the vertex at τ's largest plane angle. Let n_τ be a vector normal to τ, directed so that $\angle(n_v, n_\tau) \leq 90°$. Let $s = |vu| = |v'u| = |v''u| = |wu|$ and suppose that $s \leq 0.4132\,\mathrm{lfs}(v)$ and $s \leq 0.4132\,\mathrm{lfs}(w)$.*

Then $\angle(n_u, n_\tau) < 90°$ and $\angle(n_v, n_\tau) < 90°$. Equivalently, $n_u \cdot n_\tau$ and $n_v \cdot n_\tau$ are positive.

The proof of Lemma 16 is much like that of Lemma 15; see the full-length paper [32].

The final lemma shows that a nonempty intersection of two restricted Voronoi cells is either a lone restricted Voronoi vertex (a "degenerate" case where four or more restricted Voronoi cells share a restricted Voronoi vertex, whereas the common case is three cells sharing a vertex) or a lone topological interval justifying the name "restricted Voronoi edge."

▶ **Lemma 17.** *Let $\mathrm{Vor}|_\Sigma V$ be a restricted Voronoi diagram that satisfies all the conditions of Lemma 12, including the condition that at least three sites in V lie on each connected component of Σ. Suppose that closed ball property D and generic intersection properties E and F hold: no vertex of $\mathrm{Vor}\,V$ lies on Σ, and no edge and no 2-face of $\mathrm{Vor}\,V$ intersects Σ tangentially. Suppose also that for every restricted Voronoi vertex $u \in \mathrm{Vor}|_\Sigma V$, either*

- $|vu| \leq 0.3245\,\mathrm{lfs}(u)$ *for every site v such that $u \in \mathrm{Vor}|_\Sigma v$, or*
- $|vu| \leq 0.4132\,\mathrm{lfs}(v)$ *for every site v such that $u \in \mathrm{Vor}|_\Sigma v$.*

Let $v, w \in V$ be two distinct sites, let $F = \mathrm{Vor}\,v \cap \mathrm{Vor}\,w$, and let $f = \mathrm{Vor}|_\Sigma v \cap \mathrm{Vor}|_\Sigma w = F \cap \Sigma$.

Then one of these three claims holds: f is empty; f is a lone point (a restricted Voronoi vertex) and F is an edge; or f is homeomorphic to a closed interval and F is a 2-face.

Proof. Suppose f is nonempty. By Lemma 12, f is a union of disjoint topological intervals and isolated points. As f is nonempty and no vertex of $\mathrm{Vor}\,V$ lies on Σ (closed ball property D), F is not a vertex of $\mathrm{Vor}\,V$. Hence F is either an edge or a 2-face of $\mathrm{Vor}\,V$. If F is a Voronoi edge, then F is the intersection of three or more Voronoi cells and thus f is the intersection of three or more restricted Voronoi cells; so by assumption (the conditions of Lemma 12), f is a lone restricted Voronoi vertex and the result holds.

Only the case where F is a 2-face of $\mathrm{Vor}\,V$ remains. As closed ball property D and generic intersection properties E and F hold, $\Sigma \cap F$ cannot contain any isolated points; so f is a union of disjoint topological intervals. By Lemma 12, each interval contains exactly two restricted Voronoi vertices, its endpoints. Both of them lie on the boundary of F.

Let n_v be an outside-facing vector normal to Σ at v. We will see shortly that F is not perpendicular to n_v. Assign a direction to each edge of F such that the angle between n_v and each directed edge is at most 90°, as illustrated in Figure 6. As F is a convex polygon, we thus partition its edges into two chains, each monotone in the direction n_v. (An edge perpendicular to n_v – there are at most two – can be assigned to either chain.)

Let u be a restricted Voronoi vertex on an edge e of F. Let τ be u's dual restricted Delaunay triangle (or polygon) with vertices v and w. Let n_τ be a vector that points in the same direction as e, and observe that n_τ is normal to τ and $\angle(n_v, n_\tau) \leq 90°$. By Lemma 15 or Lemma 16, $\angle(n_u, n_\tau) < 90°$ and $\angle(n_v, n_\tau) < 90°$. The latter implies that F is not perpendicular to n_v (as promised). The former implies that as one walks along one of the directed monotone chains, one might encounter a restricted Voronoi vertex where the chain passes from inside Σ to outside Σ, but not from outside to inside. Therefore, there can be only one restricted Voronoi vertex on each chain, and only two restricted Voronoi vertices on F. It follows that $\mathrm{Vor}|_\Sigma v \cap \mathrm{Vor}|_\Sigma w$ is just a single topological interval. ◀

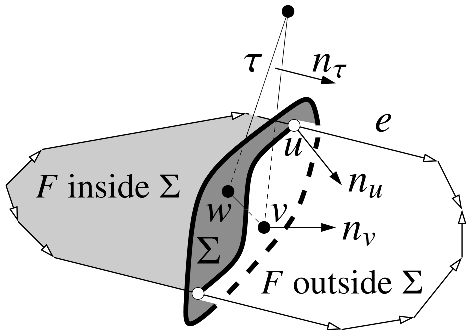

Figure 6 A Voronoi 2-face F, with its edges partitioned into two chains monotone in n_v.

7 The restricted Delaunay triangulation is homeomorphic to Σ

We conclude with homeomorphism theorems for 0.3245-samples and 0.4132-Voronoi samples.

► **Theorem 18.** *Let V be a finite ϵ-sample of Σ for some $\epsilon \leq 0.3245$. Suppose that no vertex of the three-dimensional Voronoi diagram* $\mathrm{Vor}\,V$ *lies on Σ. Then the underlying space of the restricted Delaunay triangulation, $|\mathrm{Del}|_\Sigma V|$, is homeomorphic to Σ.*

Proof. Corollary 9 guarantees closed ball property A and generic intersection property E. Corollary 11 guarantees closed ball property C and generic intersection property F. Closed ball property D holds by assumption. By Corollary 9, every connected component of Σ has at least six sites on it and no restricted Voronoi cell intersects the interior of another; all the preconditions of Lemmas 12 and 17 are satisfied. Lemma 17 guarantees closed ball property B. As Σ and V satisfy the preconditions A–F of the Topological Ball Theorem [23], $|\mathrm{Del}|_\Sigma V|$ is homeomorphic to Σ. ◄

► **Theorem 19.** *Let V be a finite ϵ-Voronoi sample of Σ for some $\epsilon \leq 0.4132$. Suppose that no vertex of the three-dimensional Voronoi diagram* $\mathrm{Vor}\,V$ *lies on Σ. Then the underlying space of the restricted Delaunay triangulation, $|\mathrm{Del}|_\Sigma V|$, is homeomorphic to Σ.*

Proof. Identical to the proof of Theorem 18, except that Corollary 9 is replaced by Theorem 6 and Lemmas 2, 7, and 5; and Corollary 11 is replaced by Lemma 10. ◄

References

1 Nina Amenta and Marshall W. Bern. Surface Reconstruction by Voronoi Filtering. *Discrete & Computational Geometry*, 22(4):481–504, June 1999. `doi:10.1007/PL00009475`.

2 Nina Amenta, Marshall W. Bern, and David Eppstein. The Crust and the β-Skeleton: Combinatorial Curve Reconstruction. *Graphical Models and Image Processing*, 60(2):125–135, March 1998. `doi:10.1006/gmip.1998.0465`.

3 Nina Amenta, Sunghee Choi, Tamal K. Dey, and Naveen Leekha. A Simple Algorithm for Homeomorphic Surface Reconstruction. *International Journal of Computational Geometry and Applications*, 12(1–2):125–141, 2002. `doi:10.1142/S0218195902000773`.

4 Dominique Attali and André Lieutier. Geometry-Driven Collapses for Converting a Čech Complex into a Triangulation of a Nicely Triangulable Shape. *Discrete & Computational Geometry*, 54(4):798–825, December 2015. `doi:10.1007/s00454-015-9733-7`.

5 Håvard Bakke Bjerkevik. Tighter Bounds for Reconstruction from ϵ-Samples. In Xavier Goaoc and Michael Kerber, editors, *38th International Symposium on Computational Geometry*, volume 224 of *Leibniz International Proceedings in Informatics (LIPIcs)*, pages 9:1–9:17, Berlin, Germany, June 2022. Schloss Dagstuhl – Leibniz-Zentrum für Informatik. `doi:10.4230/LIPIcs.SoCG.2022.9`.

6 Jean-Daniel Boissonnat, Frédéric Chazal, and Mariette Yvinec. *Geometric and Topological Inference*, volume 57. Cambridge University Press, September 2018. doi:10.1017/9781108297806.

7 Jean-Daniel Boissonnat, Ramsay Dyer, and Arijit Ghosh. Delaunay Triangulation of Manifolds. *Foundations of Computational Mathematics*, 18(2):399–431, April 2018. doi:10.1007/s10208-017-9344-1.

8 Jean-Daniel Boissonnat, Ramsay Dyer, Arijit Ghosh, André Lieutier, and Mathijs Wintraecken. Local Conditions for Triangulating Submanifolds of Euclidean Space. *Discrete & Computational Geometry*, 66(2):666–686, September 2021. doi:10.1007/s00454-020-00233-9.

9 Jean-Daniel Boissonnat, Ramsay Dyer, Arijit Ghosh, and Nikolay Martynchuk. An Obstruction to Delaunay Triangulations in Riemannian Manifolds. *Discrete & Computational Geometry*, 59(1):226–237, January 2018. doi:10.1007/s00454-017-9908-5.

10 Jean-Daniel Boissonnat and Arijit Ghosh. Manifold Reconstruction Using Tangential Delaunay Complexes. *Discrete & Computational Geometry*, 51(1):221–267, January 2014. doi:10.1007/s00454-013-9557-2.

11 Jean-Daniel Boissonnat, Leonidas J. Guibas, and Steve Y. Oudot. Manifold Reconstruction in Arbitrary Dimensions Using Witness Complexes. *Discrete & Computational Geometry*, 42(1):37–70, July 2009. doi:10.1007/s00454-009-9175-1.

12 Jean-Daniel Boissonnat and Steve Oudot. Provably Good Surface Sampling and Approximation. In *Symposium on Geometry Processing*, pages 9–18. Eurographics Association, June 2003. doi:10.2312/SGP/SGP03/009-019.

13 Jean-Daniel Boissonnat and Steve Oudot. Provably Good Sampling and Meshing of Surfaces. *Graphical Models*, 67(5):405–451, September 2005. doi:10.1016/j.gmod.2005.01.004.

14 Dobrina Boltcheva and Bruno Lévy. Surface Reconstruction by Computing Restricted Voronoi Cells in Parallel. *Computer-Aided Design*, 90:123–134, September 2017. doi:10.1016/j.cad.2017.05.011.

15 Ho-Lun Cheng, Tamal Krishna Dey, Herbert Edelsbrunner, and John Sullivan. Dynamic Skin Triangulation. *Discrete & Computational Geometry*, 25(4):525–568, December 2001. doi:10.1007/s00454-001-0007-1.

16 Siu-Wing Cheng, Tamal Krishna Dey, and Edgar A. Ramos. Manifold Reconstruction from Point Samples. In *Proceedings of the Sixteenth Annual Symposium on Discrete Algorithms*, pages 1018–1027, Vancouver, British Columbia, Canada, January 2005. URL: http://dl.acm.org/citation.cfm?id=1070432.1070579.

17 Siu-Wing Cheng, Tamal Krishna Dey, Edgar A. Ramos, and Tathagata Ray. Sampling and Meshing a Surface with Guaranteed Topology and Geometry. *SIAM Journal on Computing*, 37(4):1199–1227, 2007. doi:10.1137/060665889.

18 Siu-Wing Cheng, Tamal Krishna Dey, and Jonathan Richard Shewchuk. *Delaunay Mesh Generation*. Chapman and Hall / CRC Computer and Information Science Series. CRC Press, Boca Raton, Florida, 2013. URL: http://www.crcpress.com/product/isbn/9781584887300.

19 David Cohen-Steiner, André Lieutier, and Julien Vuillamy. Lexicographic Optimal Homologous Chains and Applications to Point Cloud Triangulations. In Sergio Cabello and Danny Z. Chen, editors, *36th International Symposium on Computational Geometry*, volume 164 of *Leibniz International Proceedings in Informatics (LIPIcs)*, pages 32:1–32:17. Schloss Dagstuhl – Leibniz-Zentrum für Informatik, 2020. doi:10.4230/LIPIcs.SoCG.2020.32.

20 Tamal Krishna Dey. *Curve and Surface Reconstruction: Algorithms with Mathematical Analysis*. Cambridge University Press, New York, 2007. doi:10.1017/CBO9780511546860.

21 Ramsay Dyer, Hao Zhang, and Torsten Möller. Delaunay Mesh Construction. In *Proceedings of the Fifth Symposium on Geometry Processing*, pages 273–282. Eurographics Association, July 2007. doi:10.2312/SGP/SGP07/273-282.

22 Ramsay Dyer, Hao Zhang, and Torsten Möller. Surface Sampling and the Intrinsic Voronoi Diagram. *Computer Graphics Forum*, 27(5):1393–1402, July 2008. doi:10.1111/j.1467-8659.2008.01279.x.

23 Herbert Edelsbrunner and Nimish R. Shah. Triangulating Topological Spaces. *International Journal of Computational Geometry and Applications*, 7(4):365–378, August 1997. `doi:10.1142/S0218195997000223`.

24 Marc Khoury and Jonathan Richard Shewchuk. Fixed Points of the Restricted Delaunay Triangulation Operator. In Sándor P. Fekete and Anna Lubiw, editors, *32nd International Symposium on Computational Geometry*, volume 51 of *Leibniz International Proceedings in Informatics (LIPIcs)*, pages 47:1–47:15, Boston, Massachusetts, June 2016. Schloss Dagstuhl – Leibniz-Zentrum für Informatik. `doi:10.4230/LIPIcs.SOCG.2016.47`.

25 Marc Khoury and Jonathan Richard Shewchuk. Approximation Bounds for Interpolation and Normals on Triangulated Surfaces and Manifolds, November 2019. `arXiv:1911.03424`.

26 Marc Khoury and Jonathan Richard Shewchuk. Restricted Constrained Delaunay Triangulations. In Kevin Buchin and Éric Colin de Verdière, editors, *37th International Symposium on Computational Geometry*, volume 189 of *Leibniz International Proceedings in Informatics (LIPIcs)*, pages 49:1–49:16, Buffalo, New York, June 2021. Schloss Dagstuhl – Leibniz-Zentrum für Informatik. `doi:10.4230/LIPIcs.SoCG.2021.49`.

27 Jisu Kim, Jaehyeok Shin, Frédéric Chazal, Alessandro Rinaldo, and Larry A. Wasserman. Homotopy Reconstruction via the Cech Complex and the Vietoris-Rips Complex. In Sergio Cabello and Danny Z. Chen, editors, *36th International Symposium on Computational Geometry*, volume 164 of *Leibniz International Proceedings in Informatics (LIPIcs)*, pages 54:1–54:19. Schloss Dagstuhl – Leibniz-Zentrum für Informatik, 2020. `doi:10.4230/LIPIcs.SoCG.2020.54`.

28 Gregory Leibon. *Random Delaunay Triangulations, the Thurston–Andreev Theorem, and Metric Uniformization*. PhD thesis, University of California at San Diego, San Diego, California, 1999.

29 Partha Niyogi, Stephen Smale, and Shmuel Weinberger. Finding the Homology of Submanifolds with High Confidence from Random Samples. *Discrete & Computational Geometry*, 39(1–3):419–441, March 2008. `doi:10.1007/s00454-008-9053-2`.

30 Nicholas M. Patrikalakis and Takashi Maekawa. *Shape Interrogation for Computer Aided Design and Manufacturing*. Springer, 2002. `doi:10.1007/978-3-642-04074-0`.

31 Jeanne Pellerin, Bruno Lévy, and Guillaume Caumon. Toward Mixed-Element Meshing Based on Restricted Voronoi Diagrams. *Procedia Engineering*, 82:279–290, 2014. `doi:10.1016/j.proeng.2014.10.390`.

32 Jonathan Richard Shewchuk. Better Sampling Bounds for Restricted Delaunay Triangulations and a Star-Shaped Property for Restricted Voronoi Cells, March 2026. `arXiv:2603.19826`.

33 Wilson A. Sutherland. *Introduction to Metric and Topological Spaces*. Oxford University Press, second edition, 2009. `doi:10.1093/oso/9780199563074.001.0001`.

34 Pengfei Wang, Zixiong Wang, Shiqing Xin, Xifeng Gao, Wenping Wang, and Changhe Tu. Restricted Delaunay Triangulation for Explicit Surface Reconstruction. *ACM Transactions on Graphics*, 41(5):180:1–180:20, October 2022. `doi:10.1145/3533768`.

35 Dong-Ming Yan, Bruno Lévy, Yang Liu, Feng Sun, and Wenping Wang. Isotropic Remeshing with Fast and Exact Computation of Restricted Voronoi Diagram. *Computer Graphics Forum*, 28(5):1445–1454, 2009. `doi:10.1111/j.1467-8659.2009.01521.x`.